DEVELOPMENT OF β-SiC/Si(100) HYDROGEN GAS SENSOR

By

Dinesh Kumar Penigalapati

Problem Report submitted to the College of Engineering and Mineral Resources
At West Virginia University
In partial fulfillment of the requirements
for the degree of

Master of Science
In
Electrical Engineering

Dimitris Korakakis, Ph.D., Chair
Charter D. Stinespring, Ph.D.
Parviz Famouri, Ph.D.

Lane Department of Computer Science and Electrical Engineering
Morgantown, West Virginia

2007

ABSTRACT

Development of β-SiC/Si(100) Hydrogen Gas Sensor

Dinesh Kumar Penigalapati

Silicon Carbide based electronic devices are well suited for high temperature application like gas sensors due to its high band gap, breakdown field, melting point and thermal conductivity. Nano thin β-SiC films have been grown on Si(100) by Gas Source Molecular Beam Epitaxy. The typical thickness of Silicon Carbide film grown is 30nm. These nano films have been used in the fabrication of Metal-Semiconductor-Metal (MSM) devices formed using aluminum Schottky contacts. The unique property of these Metal-Semiconductor-Metal devices is that the dominant conduction path does not occur at the β-SiC/Si interface, but with in entire β-SiC layer due to its small thickness. Since the conduction path depends on the surface condition of the device, these nano-thin, β-SiC films can be used in chemical agent sensors. The device was tested by keeping it in presence of Argon at 50^0C and increasing hydrogen concentration from 0% to 100% in steps of five. Resultant discussion and explanation are given.

ACKNOWLEDGEMENTS

I would like to express my deepest appreciation and gratitude to my advisor, Dr. Dimitris Korakakis, for giving me this opportunity. His knowledge and encouragement have been of great value throughout the course of my research.

I wish to express my sincere thanks to the members of my committee, Dr. Charter Stinespring and Dr. Parviz Famouri. Their understanding and constructive comments have been important throughout this work.

I owe a sincere gratitude to Dr. Kolin Brown, for his knowledge and assistance in semiconductor fabrication.

My special thanks to my SiC gas sensor teammates: Ronak Rahimi, Nick Shelton, Lee Rodak, Andrew Woodworth, Srikanth Raghavan, Tobias Denig and Christopher Miller for their interesting discussions and important work.

.

Lastly, I owe my sincere thanks to all my colleagues in the Materials Growth and Characterization Lab (MgCl) and Lane Department of Computer Science and Electrical Engineering (LDCSEE) for their valuable advice and friendly help over the course of my research.

TABLE OF CONTENTS

LIST OF FIGURES

LIST OF TABLES

Chapter 1: Introduction

Silicon Carbide based electronic devices and circuits are being developed for use in high temperature, high power and high radiation conditions under which conventional semiconductors cannot function. High temperature extreme environment solid-state gas sensing is of great interest to the automotive, aerospace and chemical processing industries. The wide bandgap, high thermal conductivity, thermal and chemical stability make silicon carbide an ideal solid-state gas sensing material for operation under harsh conditions. However, most of these operational benefits of silicon carbide have yet to be realized in actual systems, primarily owing to the fact that the growth techniques of Silicon Carbide are relatively immature and device fabrication technologies are not yet sufficiently developed to the degree required for wide spread, reliable commercial use.

Selectivity, reversibility, response time, sensitivity and operation temperature range are the factors that determine the sensor performance. With recent advancement in silicon carbide, SiC based hydrogen sensors have good selectivity, reversibility, fast response time, operated to temperature range of 600^{o}C and high sensitivity

This work proposes a new approach of solid state gas sensors for the detection of hydrocarbon gases. The resultant background information pertaining to semiconductor physics, fabrication, and the electrical characterization of devices are provided. Various issues that were encountered and the approaches followed for resolving these obstacles are discussed. Achievements include the growth of nano-thin β-SiC layers on Si substrates, the electrical characterization of films, SiC response at higher temperatures and SiC response to different concentration of hydrogen.

Chapter 2: Silicon Carbide

2.1 Overview

In this chapter, material properties, polytypes, electronic benefits and high temperature effects of silicon carbide are presented.

2.2 Introduction

Silicon Carbide is a wide band physically robust semiconductor whose crystal lattice is cross between pure silicon and diamond. Silicon is the foundation of the modern microelectronics industry, and is perhaps the most highly developed manufacturing technology in the history of mankind. Semiconducting diamond has electronic properties far superior to silicon, but it has not been developed commercially because its extreme material stability makes ordinary semiconductor fabrication techniques impractical. The perfect cross between silicon and diamond is silicon carbide. Silicon carbide crystal lattice is identical to silicon and diamond, but exactly half the lattice sites are occupied by silicon atoms and half by carbon atoms. Silicon carbide electronic properties are superior to silicon like diamond.

Silicon Carbide based electronic devices and circuits are especially suitable for high-temperature, high-power, and high radiation environments because of its high bandgap energy. The band gap of silicon carbide is about three times greater than silicon. But the average density of electron-hole pair in silicon carbide is sixteen orders of magnitude lower than silicon at room temperature. Also the thermal leakage current (dark current) in silicon carbide is sixteen orders of magnitude lower than silicon.

2.3 Polytypism in Silicon Carbide

Silicon carbide occurs in many different crystal structures called polytypes. While there are over 100 known polytypes of silicon carbide, only a few are commonly grown in a reproducible form

acceptable for use as semiconductors. The most common polytypes of silicon carbide being developed for electronics are 3C-SiC, 4H-SiC, 6H-SiC. 3C-SiC, also referred as β-SiC, is the only form of silicon carbide with a cubic crystal structure. The non cubic polytypes of Silicon carbide are referred as α-SiC. 4H-SiC and 6H-Sic are polytypes with a hexagonal crystal structure. Though all silicon carbide polytypes chemically consist of 50% carbon atoms covalently bonded with 50% silicon atoms, each SiC polytype has its own distinct set of electronic properties. [**Powell, 2002**]

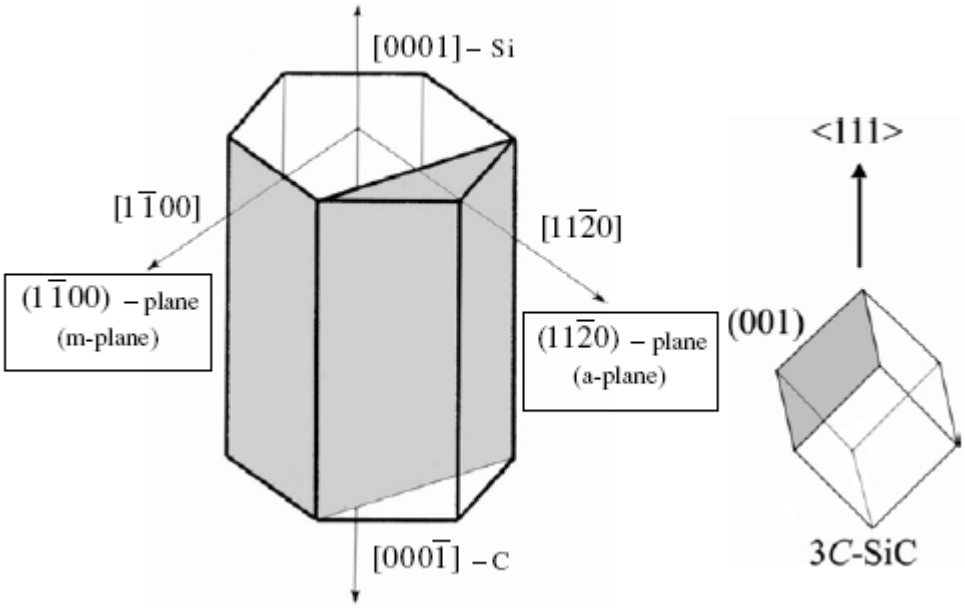

Figure 2.1 – Schematic images of the hexagonal and cubic crystal lattice of SiC [Lebedev, 2006]

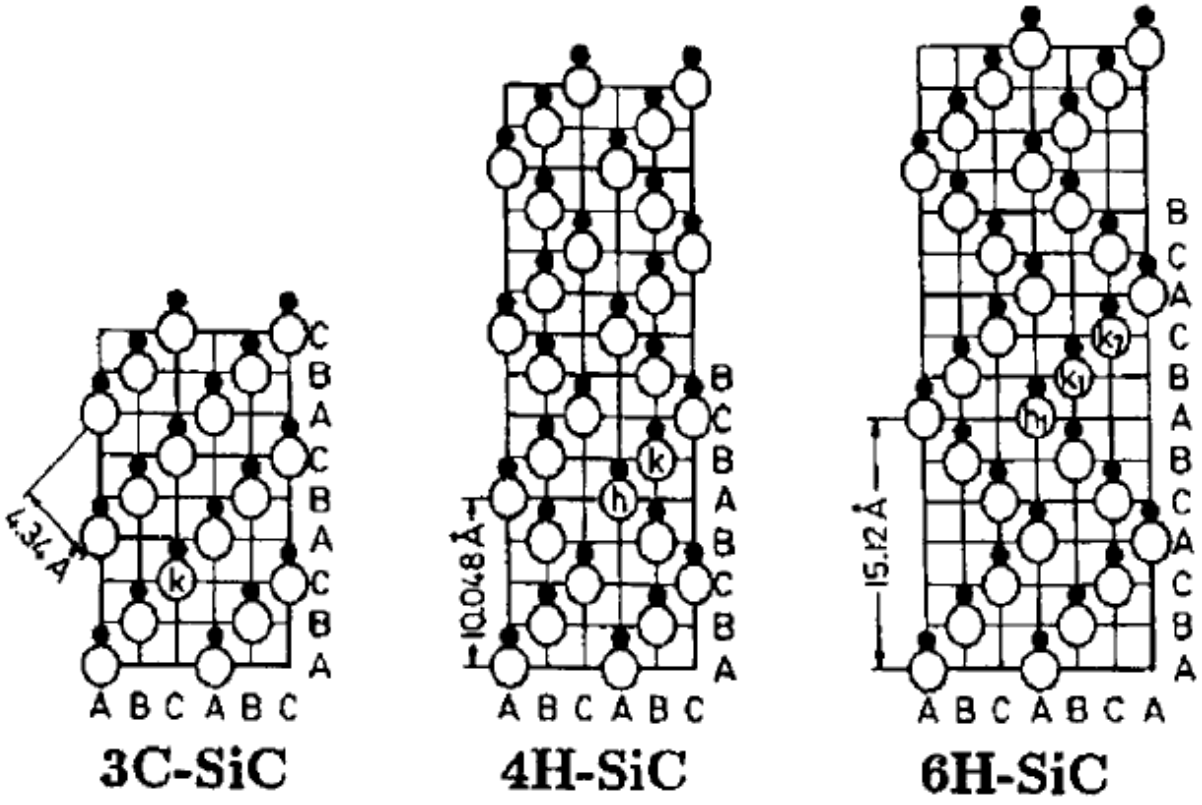

Figure 2.2 – Positions of Si and C atoms for different SiC polytypes[Lebedev, 2006]

Owing to different arrangement of silicon and carbon atoms within the Silicon Carbide crystal lattice, each SiC polytype exhibits unique electrical and optical properties. Some of the more important semiconductor electrical properties of 3C, 4H and 6H silicon carbide polytypes at room temperature are given in Table 2.1. Even with in a given polytype, some important electrical properties are non isotropic, in that they are strong function of crystallographic directions of current flow and applied electric field (e.g., electron mobility of 6H-SiC).

Silicon Carbide					
Table 2.1 **[Neudeck, 2001]**					
Comparison of properties of Silicon Carbide polytypes, Silicon and GaAs at 300K.					
Property	Silicon	GaAs	4H-SiC	6H-SiC	3C-SiC
Bandgap (eV)	1.1	1.42	3.2	3.0	2.3
Breakdown Field, $N_D=10^{17}$ ($MVcm^{-1}$)	0.6	0.6	3.0	3.2	1.5
Thermal Conductivity ($W\ cm^{-1}K^{-1}$)	1.5	0.5	5	5	5
Intrinsic Carrier Concentration (cm^{-3})	10^{10}	10^{6}	10^{-7}	10^{-5}	10
Electron Mobility, $N_D=10^{16}$ ($cm^2V^{-1}s^{-1}$)	1200	6500	800	400	750
Hole Mobility, $N_D=10^{16}$ ($cm^2V^{-1}s^{-1}$)	420	320	115	90	40
Saturated Electron Velocity ($10^7 cms^{-1}$)	1.0	1.2	2	2	2.5
Commercial Wafer Availability (cm)	30	15	5	5	None
Lattice Constant (Å)	5.43	5.65	3.07	3.08	4.36
Melting Point (K)	1690	1510	3000	3000	3000

Properties of Silicon were also included in Table 2.1 because silicon is the semiconductor employed in most commercial solid state electronics. Silicon is the yardstick by which other semiconductor materials must be evaluated against. The most beneficial superior material properties of silicon carbide over silicon listed in Table 2.1 are its wide bandgap energy, exceptionally high breakdown electric field, high thermal conductivity and high carrier saturation velocity.

2.4 Electronic Benefits

The low intrinsic carrier concentration and wide bandgap energy of silicon carbide allow it to maintain semiconductor behavior at much higher temperatures than silicon. Normally semiconductor electronic devices work in temperature range where intrinsic carrier concentration is negligible. So the conductivity is controlled by the intentionally introduced dopant impurities. Also the leakage current increases by very large amount as temperature increases due to the exponential increase of intrinsic carriers. At higher temperatures, semiconductor device operation is overcome by uncontrolled conductivity as intrinsic carriers exceed intentional device dopings. The smaller intrinsic carrier concentration of silicon carbide makes the device to operate successfully at 800^{o}C junction temperature, where it in silicon it is less than 300^{o}C.

The high breakdown field, high thermal conductivity and high operational junction temperature makes the device to function at extreme high power density. The higher breakdown field and wide energy bandgap of silicon carbide also enable much faster power switching (**Baliga, 1993) (Chow et al, 1998)** than is possible in volt-amp rated silicon power switching devices. So silicon carbide based power converters can operate at higher switching frequencies with much greater efficiency(less switching energy loss). This is highly desirable phenomenon because it permits use of smaller capacitors, inductors and transformers, which in turn can reduce overall system size and weight.

The high thermal conductivity of silicon carbide enables more efficient removal of waste heat energy from the active device, because heat energy radiation efficiency increases greatly with increasing temperature difference between the device and the cooling ambient. The ability of silicon carbide to operate at high junction temperatures permits much more efficient cooling to take place, so that the heat sinks and other device cooling hardware typically needed to keep high power devices from over heating can be made much smaller or even eliminates.

Chapter 3: Metal Contacts on Semiconductor

3.1 Overview

This Chapter explains about the metallic contacts on the semiconductor and presents the difference between schottky contacts and ohmic contacts. It also presents the good ohmic and schottky contacts for β-silicon carbide.

3.2 Introduction

Metal to semiconductor contacts have great importance in semiconductor devices. A semiconductor device is connected to the outside world through metallic contacts. They can be having as a schottky barrier or as an ohmic contact dependent on the characteristic of interface. These metal semiconductor junctions are characterized by the difference between the metal work function and the conduction band edge of semiconductor.

3.3 Schottky Contacts

When a metal and semiconductor are in contact, there exists a potential barrier between two that prevents carriers (electrons and holes) from passing one to other side. The difference between fermi energy level and vacuum level of a material is called work function. When a metal with work function Φ_m is in contact with semiconductor Φ_s electrons flow from the material with lower work function to the other material until their Fermi levels are aligned. So the material with lower work function attains positive charge and the other one gets negative charge. Thus they finally develop electrostatic field called built in electric field, which prevents the transfer of electrons between the two materials and acts like a potential barrier. When a bias voltage is applied to the junction the barrier will be decreased or increased, there by allowing the transfer

or blocking of charges respectively. When the junction conducts for one bias polarity and does not conduct for the other, then it is called schottky barrier or rectifying contact.

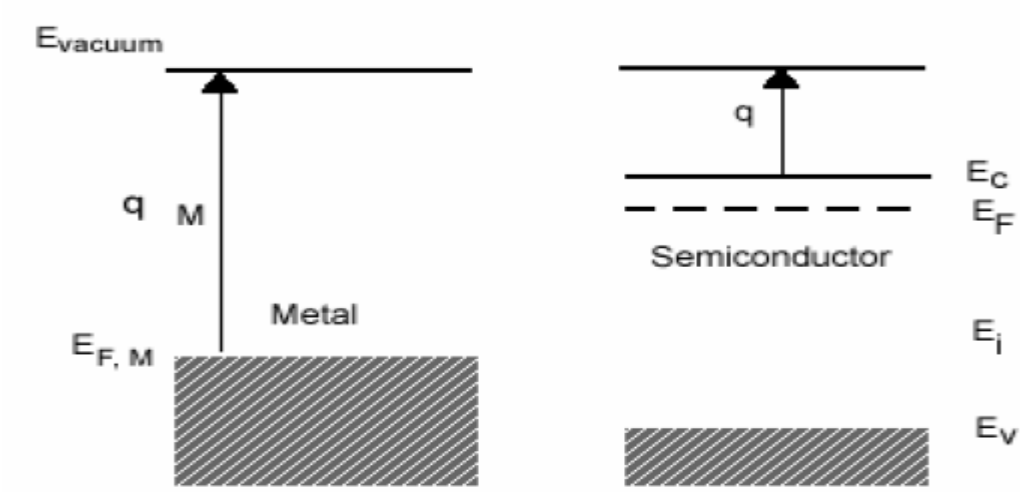

Figure 3.1 Energy band diagram of a n-type semiconductor and metal before they are made into contact.

The above figure illustrates the potential barrier of metal and n type semiconductor before they are made into contact. Once they are in contact the Fermi level of any two materials in contact must be equal. So the electrostatic potential of the semi conductor is raised to align the Fermi levels by the transfer of electrons from the semi conductor to the metal forming a depletion region of width W_o in the semiconductor.

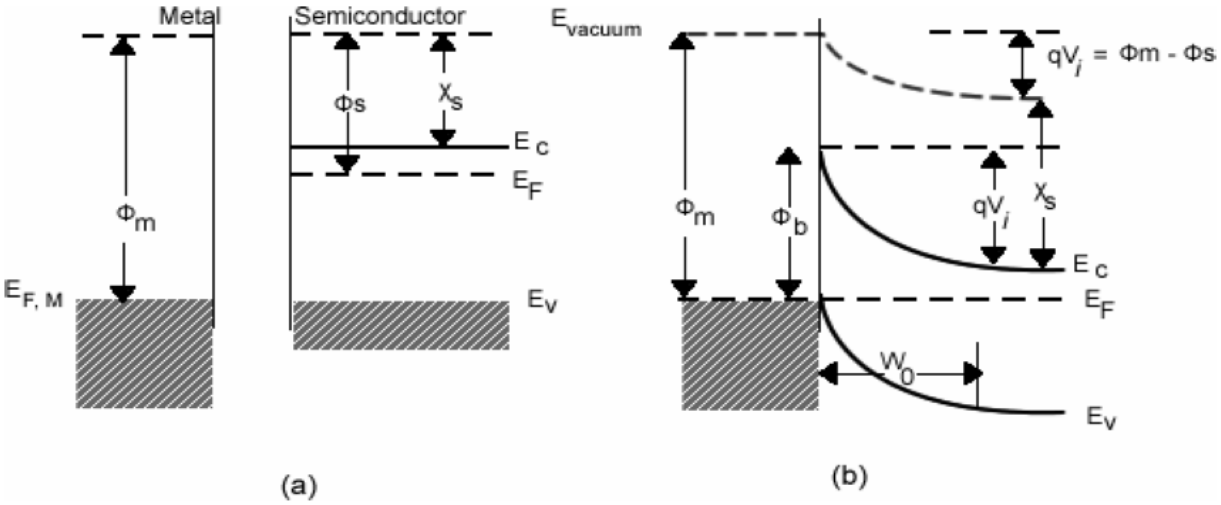

Figure 3.2 Energy band diagram of metal and semiconductor (a) before contact and (b) at thermal equilibrium after the contact is made.

The barrier height, qΦB, is defined as the potential difference between the Fermi energy of the metal and the band edge where the majority carriers reside. The barrier height on the n type semiconductor can be obtained from

$$\Phi_B = (\Phi_M - \chi_S)$$

Where $q\Phi_M$ is the work function of the metal and $q\chi_S$ is the electron affinity of the semiconductor. Electron affinity is measured from the semiconductor conducting band edge to the vacuum level.

The contact potential (Vi) prevents further transfer of electrons from the semiconductor conduction band into the metal. It is the difference between the work function of metal and the Fermi level of semiconductor.

3.3.1 Forward and Reverse bias

When a positive voltage is applied to the metal, the Fermi energy level of the metal is lowered with respect to semiconductor. This reduces the potential barrier in the semiconductor and more electrons in the semiconductor have sufficient energy to diffuse through the barrier into the metal than drifting into the semiconductor. This constitutes the positive current through the junction at a voltage comparable to the junction potential.

Under reverse bias conditions, the Fermi energy level of the metal increases with respect to semiconductor. As a result, the potential barrier in the semiconductor increases and spreads over a larger area. It prevents the diffusion of electrons from semiconductor into the metal without affecting the electrons drifting in the opposite direction which constitutes reverse bias current which is almost negligible.

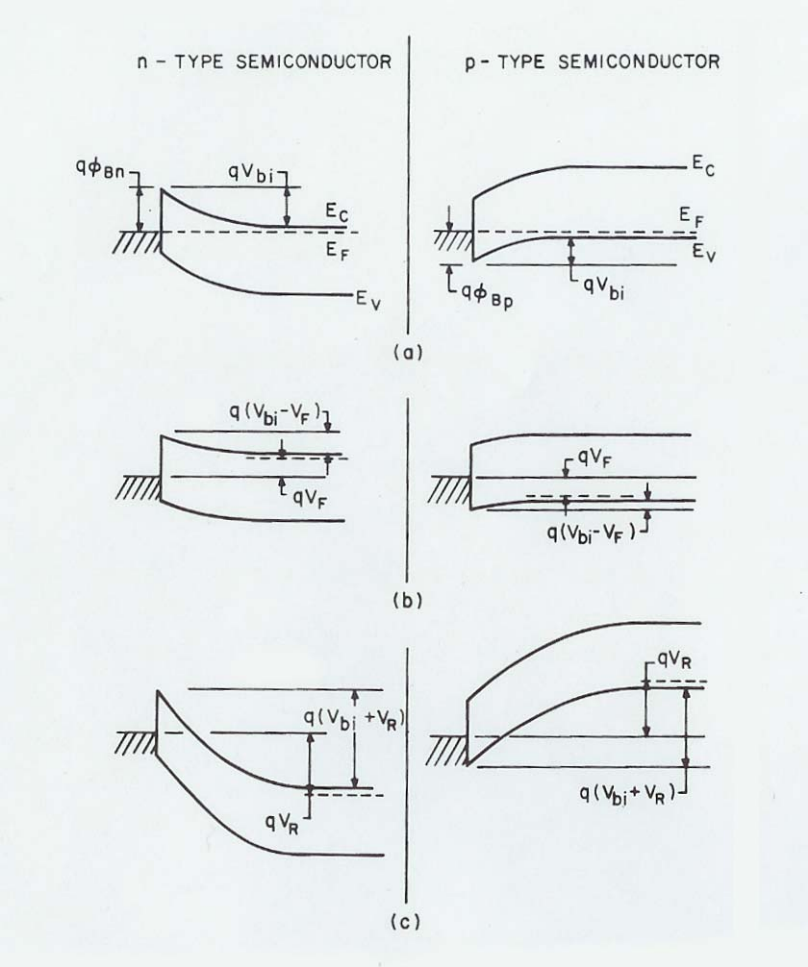

Figure 3.3 - Energy-band diagram of metal n-type and metal p-type semiconductors under different biasing conditions (a) Thermal equilibrium. (b) Forward bias. (c) Reverse bias. [Sze, 1981].

3.4 Ohmic Contacts

While the Schottky contacts conduct for one polarity, the Ohmic contacts conduct irrespective of the polarity of the applied external bias. I-V characteristic of Schottky and Ohmic constants is shown below.

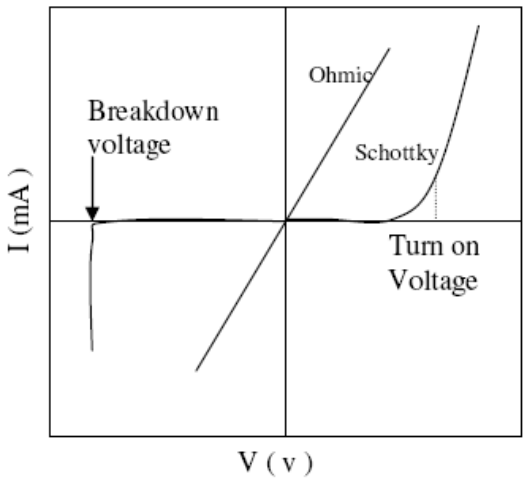

Fig. 3.4 I-V characteristics of Schottky and Ohmic contacts

A contact between a metal and semiconductor is typically a Schottky barrier. The Ohmic contact formation depends on either eliminating the Schottky barrier altogether or making the barrier sufficiently thin enough so that electrons can tunnel through. Selection of contact metal based on matching the work function of the materials may eliminate the Schottky barrier. More often than not it is not possible to find the right combination.

Instead most Ohmic contacts are formed by creating a highly doped region near the surface of the semiconductor that reduces the depletion width significantly, resulting in a tunneling Ohmic contact [Pallab, 1997].

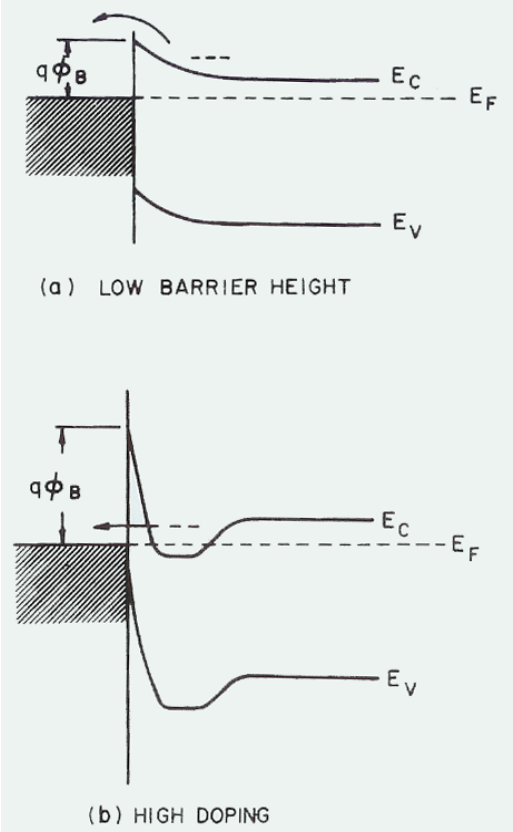

Fig. 3.5 (a) Low barrier height, (b) High doping for ohmic contacts

Generally, the resistance of the Ohmic contact has a very small resistance compared to the bulk resistance of the semiconductor. Ideal Ohmic contacts do not contribute to the voltage drop across the device and do not alter the I-V relationship. The contacts should remain intact and robust irrespective of the environment. Naturally, not all of these requirements can be met simultaneously [Morkov].

3.5 β-SiC/Si Contacts

Metals with large work functions are suitable for Schottky contacts. The work functions of various metals are given in the following table [Neamen, 1992]:

Metal	Work function (eV)
Ag	4.26
Al	4.28
Ti	4.33
Cr	4.5
W	4.55
Mo	4.6
Au	5.1
Pd	5.12
Ni	5.15
Ir	5.20
Pt	5.65

Table 3.1: Work functions of different metals [Neamen, 1992]

Platinum is proved to be good schottky contact for β-silicon carbide **[Davis, 1991].** High temperature deposition of platinum over β-silicon carbide results in formation of silicides which were uniform and highly stable for temperatures (~1300K).

Nickel acts as a good ohmic contact for β-silicon carbide **[Jin, 2006] [Wan, 2002].** At high temperatures nickel forms silicides with β-Silicon carbide which were the responsible for the good ohmic contact formation. But the disadvantage is unpredictability in controlling the Ni-SiC reaction it has become difficult to continuously yield lower contact resistance. Alloy of TiW also acts as good ohmic contact for β-Silicon carbide. **[Ohn, 2006].** These contacts were thermally stable up to 2700^{o}C with low contact resistivity.

Chapter 4: Metal Semiconductor Metal Devices

4.1 Overview

This chapter explains about the Metal–semiconductor–metal (MSM) devices, their applications in electronic field, advantages and disadvantages.

4.2 MSM devices

The metal-semiconductor-metal (MSM) devices are two terminal devices having two schottky contacts on a uniformly doped semiconductor. The properties of these MSM devices were different from a schottky diode. In these devices we can obtain minority current many orders of magnitude larger than the majority current.

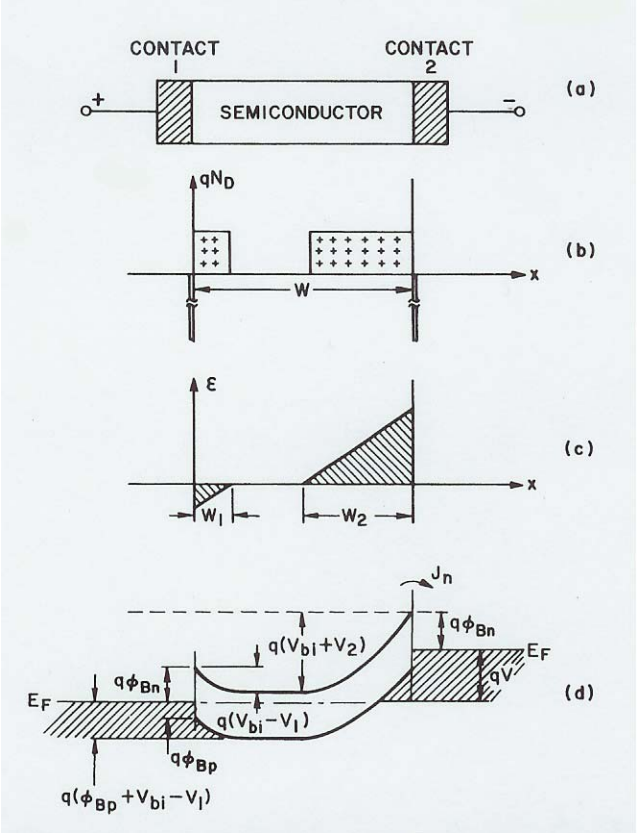

Figure 4.1 - Metal-semiconductor-metal (MSM) structure. (a) MSM with uniformly doped n-type semiconductor. (b) Charge distribution under low bias. (c) Field distribution. (d) Energy-band diagram. [Sze, 1971]

Ideally, MSM devices are symmetrical. These devices can be compared to two schottky barriers connected back to back where barriers at both contacts are equal. When voltage is applied to these MSM devices one contact is forward biased and the other is reverse biased.

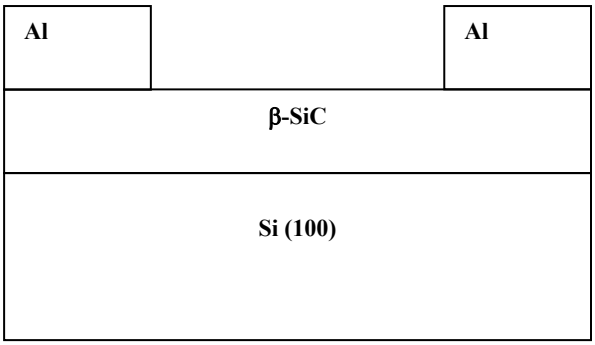

Fig 4.2. Schematic diagram of β-SiC MSM device

Now days, these MSM devices were used in photo detectors [**Naset, 2001**] [**Naset, 1997**], Barrier Injection Transit Time (BARITT) diodes [**Chu, 1971**]. The main problem with these Metal Semiconductor Metal devices was it is difficult to control these devices. But their ease of fabrication, high speed and ease of integration have generated focus of many efforts in optoelectronic research.

Chapter 5: Experimental Procedure

5.1 Overview

In this chapter presents the growth of β-silicon carbide on silicon using the gas source molecular beam epitaxy. The procedure for contacts deposition likes cleaning, contact deposition, electrical characterization were presented. Specifications of the TLM mask and procedure for surface treatment were also presented.

5.2Growth of β-SiC on Silicon

Gas source molecular beam epitaxy (GSMBE) is used to produce high quality silicon carbide films on silicon. GSMBE was operated with gaseous precursors at low temperatures. So the main advantages are low process temperature and high purity. But the disadvantages are low deposition rate and high cost of molecular beam epitaxy. The typical growth rates for MBE deposition are 0.03–0.3 Å/s. unintentionally n-doped β-SiC films were epitaxially grown (100) on n-type silicon substrate with doping density of $N_D = 10^{17.}$

Initially the silicon substrate is cleaned with a modified fenner etch. Then the sample is degreased in TCE for 10 minutes, acetone bath for 5 minutes and methanol bath for 5 minutes. A 5 minutes DI water rinse is then given to sample before it is places in a diluted solution of $NH_4OH/H_2O_2/H_2O$ (1:1:5) for 10 minutes at 80^oC. The sample is then rinse for 5 minutes in DI water and blow dried in nitrogen. A diluted bath of HF/H_2O (1:50) is given for 15 seconds followed by second diluted bath of HCl/ H_2O_2/H_2O (1:1:6) for 10 minutes and finally a 20 minutes rinse in DI water. The sample is blow dried in nitrogen and places in a dilute solution of HF/H_2O/Alcohol (1:1:10) for 2.5 min followed by a methanol rinse for 10 seconds and blow dried with nitrogen before placing the sample in the growth chamber of GSMBE.

Silicon substrate is carbonized by subjecting the sample for 800^oC for 30 minutes to reduce lattice mismatch (20%) between silicon carbide and silicon. The β-SiC layer s then grown on the

carbonized layer using dimethylsilane gas for 1 hour at 800^{o}C. The typical thickness of β-SiC layers on silicon were 30nm.

5.3 Cleaning

The β-SiC/Si samples have to be degreased before processing. The degreasing process consists of acetone bath and methanol bath. The sample has to be kept in acetone for 5 minutes and then in methanol for 5 minutes. After that samples were blown dry with nitrogen.

5.4 Contacts deposition

Once the samples are degreased they are ready for patterning. Image reversal photolithography is performed using Transmission Line Method (TLM) mask. AZ5214 photo-resist is spun on the sample for 4000 RPM for 50 seconds and then immediately baked on hot plate for 45 seconds at 90^{o}C. The sample was exposed to UV light in the mask aligner. The Appropriate exposure time was calculated depending upon the lamp test of the mask. The energy required for image reversal is 37.5mJ/cm^2 at a wavelength of 320nm. The calculated exposure time is 15 seconds. The exposed sample is post baked on the hot plate for 2 minutes at 120^{o}C. In order to reverse the patterned image, the sample must be placed in the flood exposure system. The calculated exposure time is 82 seconds. The energy required for flood exposure is between 1KJ/cm^2 to 2KJ/cm^2 at a wavelength of 365nm.The sample is then developed in the solution of AZ400K (1 part of developer: 6 parts of water) and blown dry by nitrogen.

The Sample is then places in DC sputtering station (CVC 610 magnetron sputtering machine) to deposit contacts. The power used for small targets is 0.1KW and large target is 0.4KW. Time for deposition was based on the unique deposition rate of metal. A conventional metal liftoff process was done to develop the contacts. The sample was place in acetone bath for 8 minutes and then in ultrasonic bath (which contains DI water) for few seconds. The sample was blown with acetone to remove the unnecessary metal on the sample and cleaned in methanol for 5 minutes.

After blowing nitrogen the sample was ready for characterization. Figure 5.1 shows the Al contacts on β-SiC/Si sample.

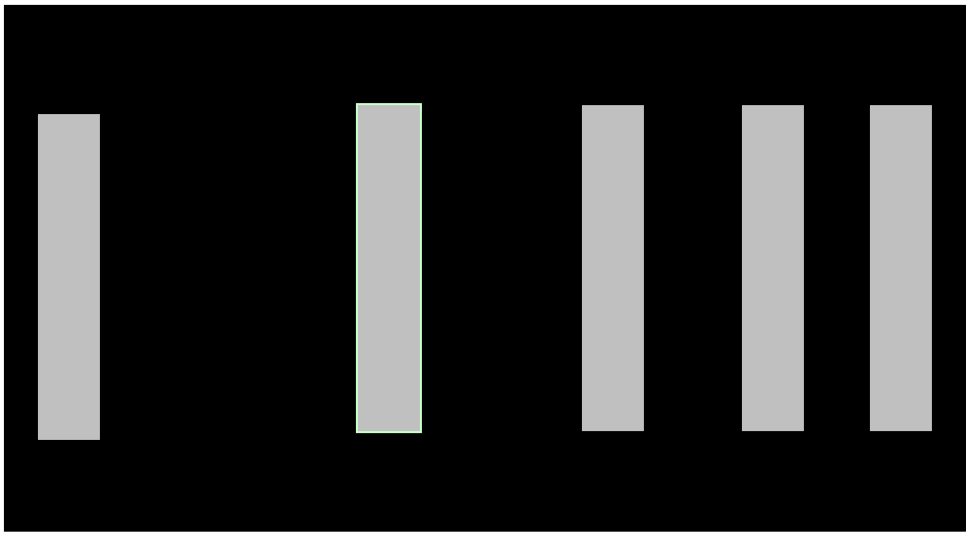

Figure 5.1 Al contacts on β-SiC/Si

5.5 Electrical Characterization

HP4145B semiconductor parameter analyzer was used to obtain the current to voltage results. This Current-Voltage results provided electrical characterization of β-SiC films. The I-V characteristics were obtained using the simple two probe technique. In this method, the probe was in contact to metal contacts. The other end of the probe was connected to voltage and current sources respectively. The semiconductor parameter analyzer was configured in diode mode. The voltage varied over a range of values and the corresponding values of current were recorded. The setup for I-V characteristics for Rectangular Transmission Line Pattern is shown below.

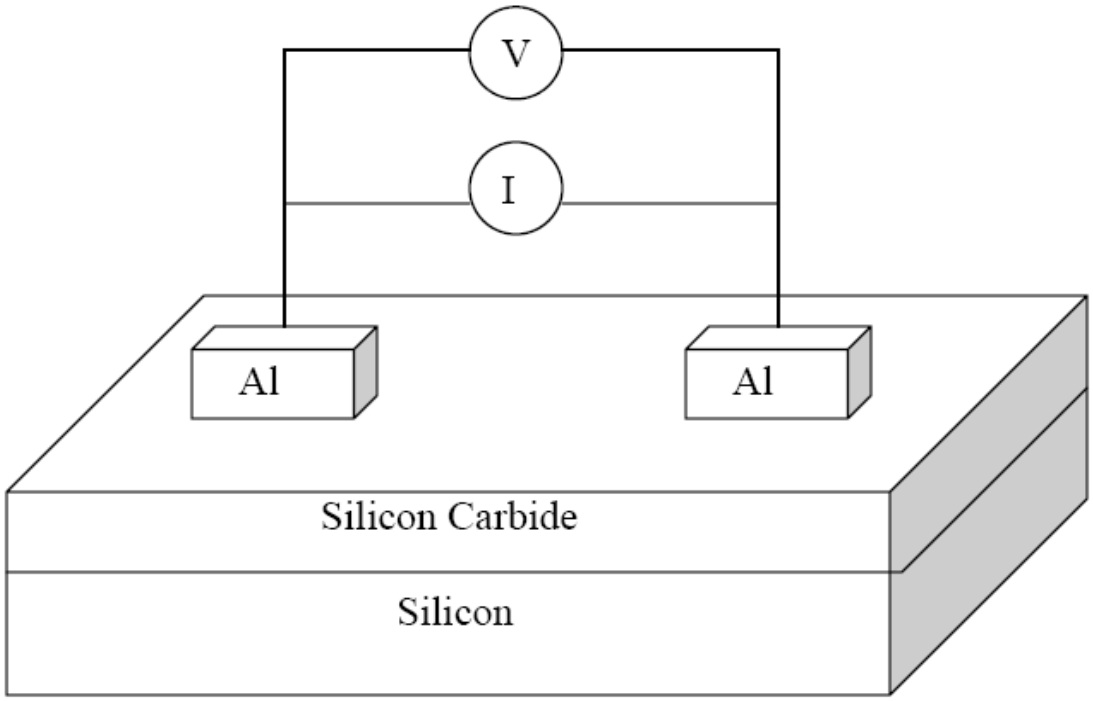

Figure 5.2 HP4145B semiconductor parameter analyzer setup

5.6 Contacts Mask

We employ Rectangular Transmission Line Method (TLM) to obtain the specific contact resistivity of the contacts. The rectangular TLM consists of rectangular pads placed at different distances. The area of rectangular pad is the same in a column. The dimensions of the pads are 400µm X 120µm, 300µm X 120µm, 300µm X 100µm, 300µm X 80µm and 200µm X 80µm. The spacing between the contacts is 30µm, 60µm, 120µm, 200µm, 300µm, 400µm, 800µm. By biasing adjacent pads, I-V characteristics can be obtained.

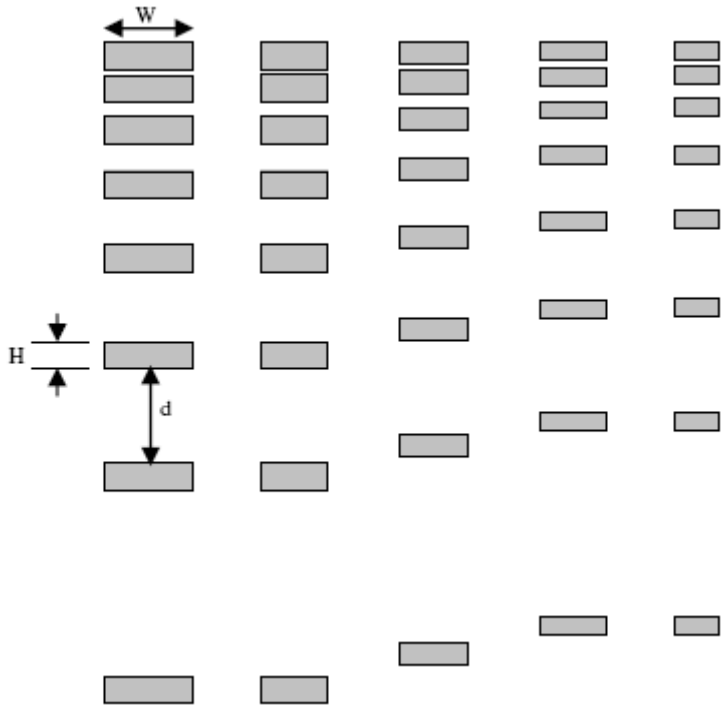

Figure 5.3 TLM mask used for contact deposition

5.7 Surface Treatment

A special surface treatment was performed on few selected samples. A 300nm SiO_2 layer was deposited on surface of β-SiC after acetone and methanol bath. Samples were then patterned following the same procedures for normal contact deposition. After development, a buffer oxide etch (H_2O: HF/10:1) was performed to remove the exposed SiO2 and expose β-SiC surface. The sample was then submitted to sputtering station for metallization.

5.8 Wire Bonding

Gold metal of thickness 600nm was deposited over the aluminum contacts for the wire bonding. The sample is attached to the bonding pad using epoxy. The thickness of gold wire used for bonding is 30μms. this gold wire connects the contacts of sample to contact pins in the bonding pad.

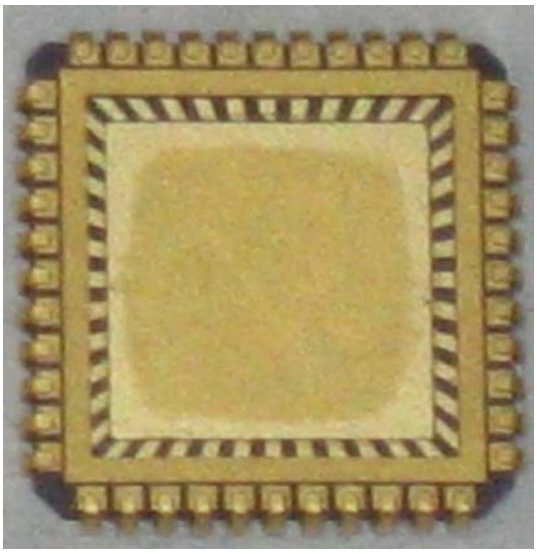

Figure 5.4 Bonding Pad

Figure 5.4 shows the bonding pad look like. WEST-Bond 747677E is used for gold wire bonding. The wire bonding takes place at a temperature 72^{o}C.

5.9 Hydrogen gas chamber setup

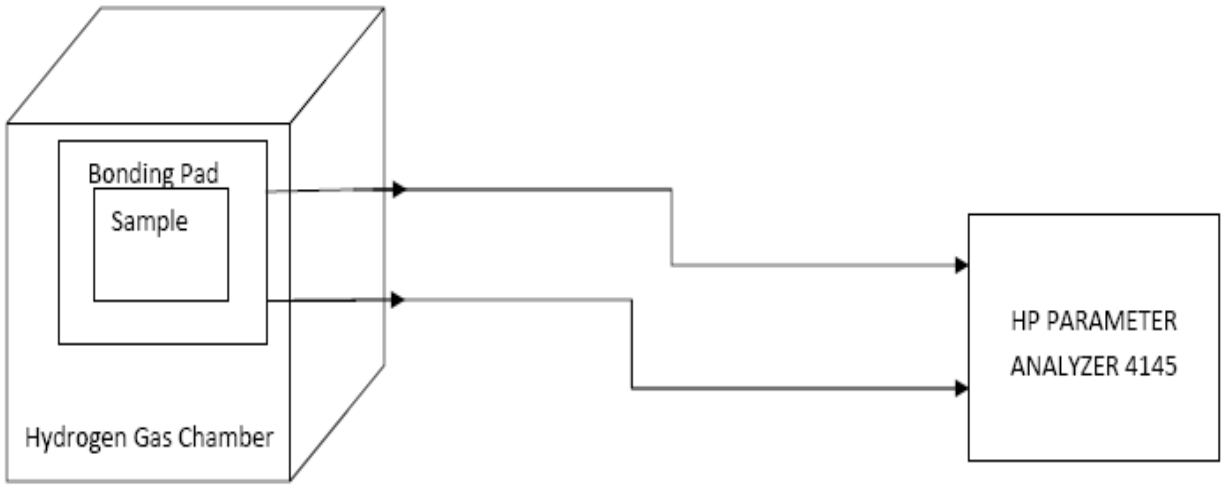

Fig 5.5. Hydrogen Chamber Setup

Fig 5.5 shows the hydrogen chamber setup for the β-SiC/Si Sample. The contacts of the bonding pads were connected to the female to male connectors. The ends of those connectors were connected to the HP parameter analyzer 4145 for measuring I-V characteristics. The sample along with the bonding pad is kept inside the hydrogen chamber. Initially chamber is pumped down to remove all the gases inside the chamber. Argon is set to flow continuously throughout the experiment. Hydrogen is set to flow from 5% to 100% in steps of five. I-V readings were taken with the help of HP parameter analyzer 4145.

Chapter 6: Experimental Results

6.1 Overview

In this chapter, results obtained from the electrical characterization of β-SiC films were presented. Explanations for those results were also given.

6.2 IV results of Bulk β-SiC/Si(100)

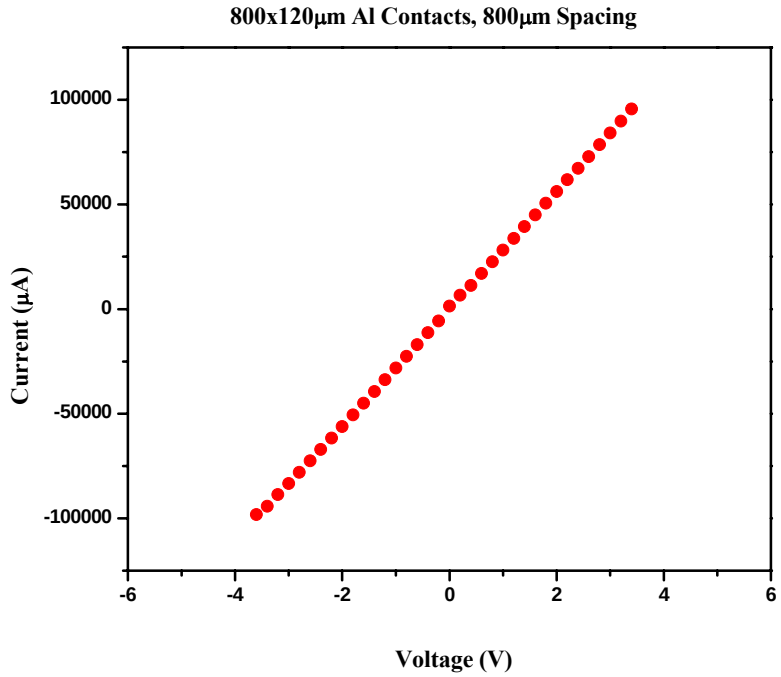

Figure 6.1 - I-V characteristics of bulk β-SiC/Si (100)

This bulk sample is obtained from the facilities of R.F. Davis from Carnegie Mellon University. Although the exact thickness of the Silicon carbide was not known, it is believed to be several microns. Aluminum contacts were deposited on this β-SiC/Si sample. Results shows that these contacts are ohmic (Fig. 6.1) in agreement with results obtained from literature. **[Basu, 2000].**

6.3 Comparison of IV results of nano-thin β-SiC/Si (100) vs. Si substrate

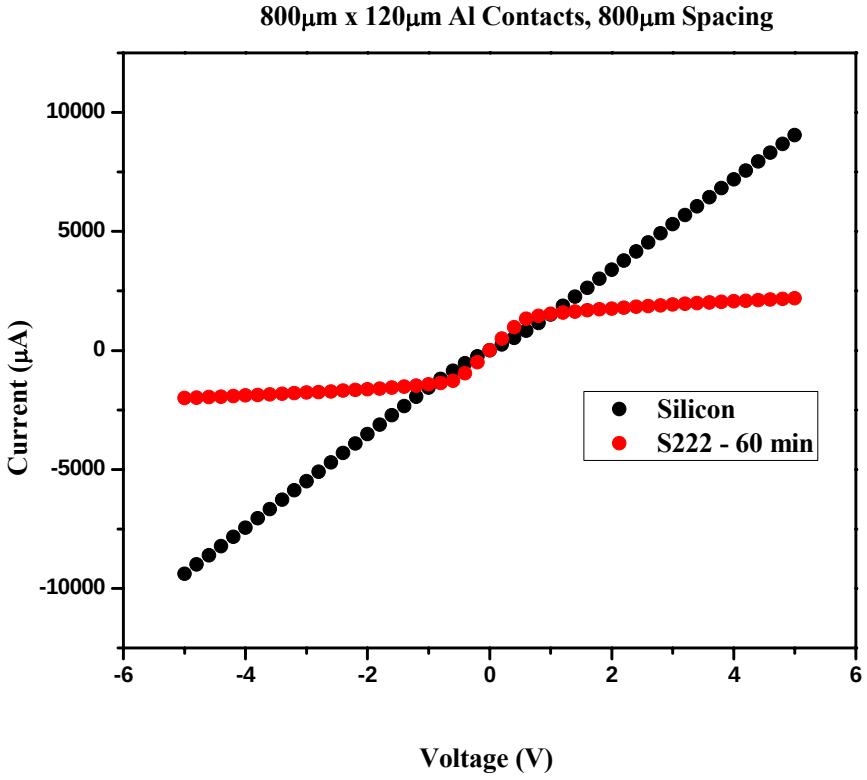

Figure 6.2- I-V characteristics of β-SiC/Si (100) Heterostructure

Figure 6.2 shows the I-V characteristics of a nano thin β- SiC/Si heterojunction. Aluminum contacts were deposited on these sample. The I-V Characteristics of these nano thin β- SiC/Si heterojunction were not ohmic like the bulk β- SiC. Besides the Aluminium on these nano thin β- SiC/Si heterojunction forms schottky contacts. When two Schottky contacts are connected back-to-back a Metal-Semiconductor-Metal (MSM) device is formed. One contact is forward-biased while the other is reverse-biased. The observed saturation current on each side of the bias represents the reverse saturation current of the opposite Schottky-barrier junction**.[Yeh, 1985].**

6.4 Comparison of IV results of β-SiC/Si (100) vs. different contact areas

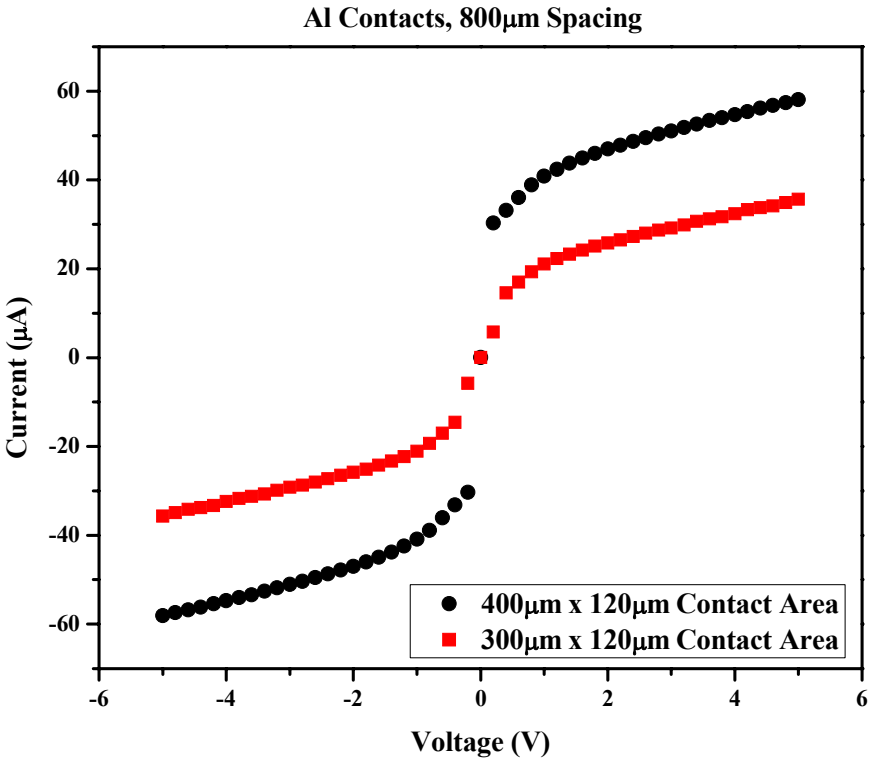

Figure 6.3 - I-V characteristics of β-SiC/Si (100) Heterostructure

The I-V characteristics of a β-SiC/Si heterojunction for different contact areas are shown in Fig. 6.3. The current obtained for 400μm x 120 μm contact was compared to be larger than the current obtained for 300μm x 120 μm because the increase in contact area lead to an increase in saturation current and an increase in the rise of current around the zero-bias region in both directions. Also electrical resistivity is inversely proportional to contact area as per agreement with electrical resistivity equation.

6.5 Comparison of IV results of nano-thin β-SiC/Si (100) under illumination

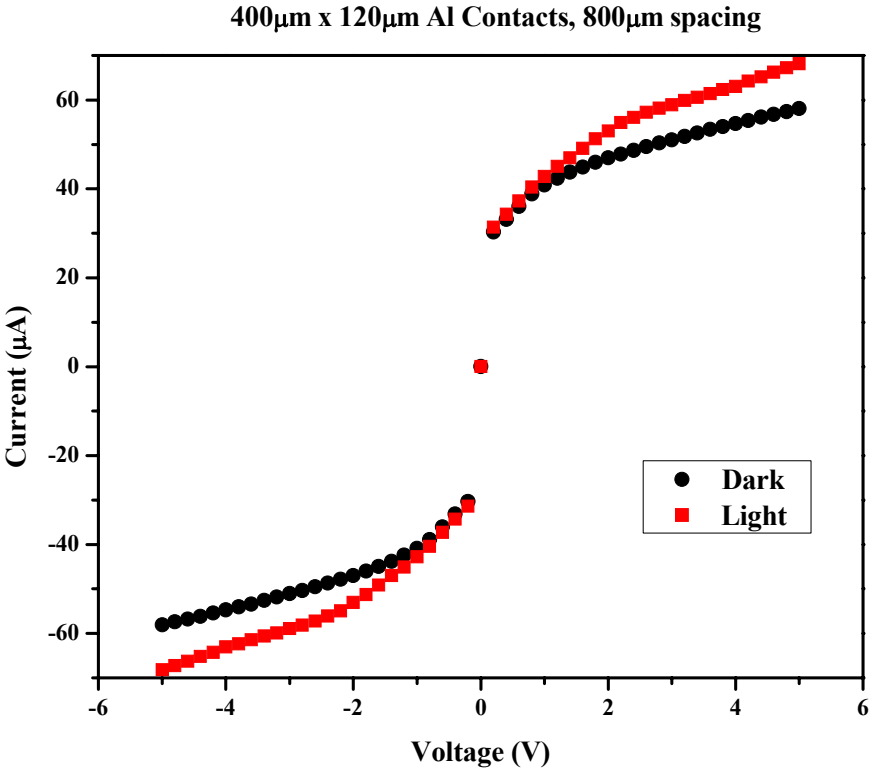

Figure 6.4 - I-V characteristics of β-SiC/Si (100) Heterostructure.

The I-V characteristics of a β-SiC/Si heterojunction when light source is present and when light source is not present are shown in Fig. 6.4. Electron-Hole-Pair (EHP) generation was important component of current in a MSM device. They may be generated due to thermal disturbances or optical disturbances. So for the investigation of optically generated Electron hole pair the sample was electrically characterized by switching on the probe station lamp. On comparing both the curves we observe at low biases in both polarities the curves remain fairly similar. But as the bias voltage increases separation also increases due to the generation of E-H pair and acts like a photo-detector **[Lu, 1993].**

6.6 Comparison of IV results vs. different growth times of nano-thin β-SiC/Si

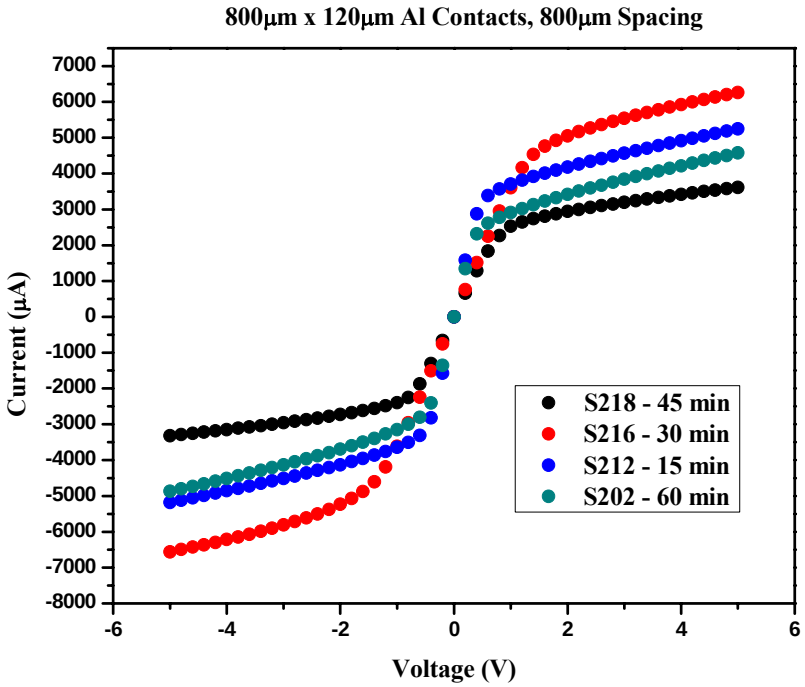

Figure 6.5 - I-V characteristics of β–SiC/Si (100) Heterostructure

The I-V characteristics of a β-SiC/Si heterojunction versus different growth times are shown in Fig 6.5. Longer growth times should yield thicker β-SiC layers, contributing to higher currents. The largest current recorded was achieved by a sample growth of 30 min and where the smallest current belong to a 45 min growth. For uniformity, the four samples were processed at the same time to eliminate any discrepancies that may occur during fabrication. The observed differences between the samples are believed to have occurred during film growths. Because the films are nano-thin (<50nm), the smallest variations in growth conditions will yield significant results in the electrical characterization of the films. Specifically, any fluctuations in temperature and gas flow will be detrimental to film quality and growth. It is believed that due to temperature variations, the film growths in question saturate before the final 60 min growth time. So it does not appear to be any consistent relationship between film thickness and growth times.

6.7 IV results of H_2 interaction on nano-thin β-SiC/Si (100)

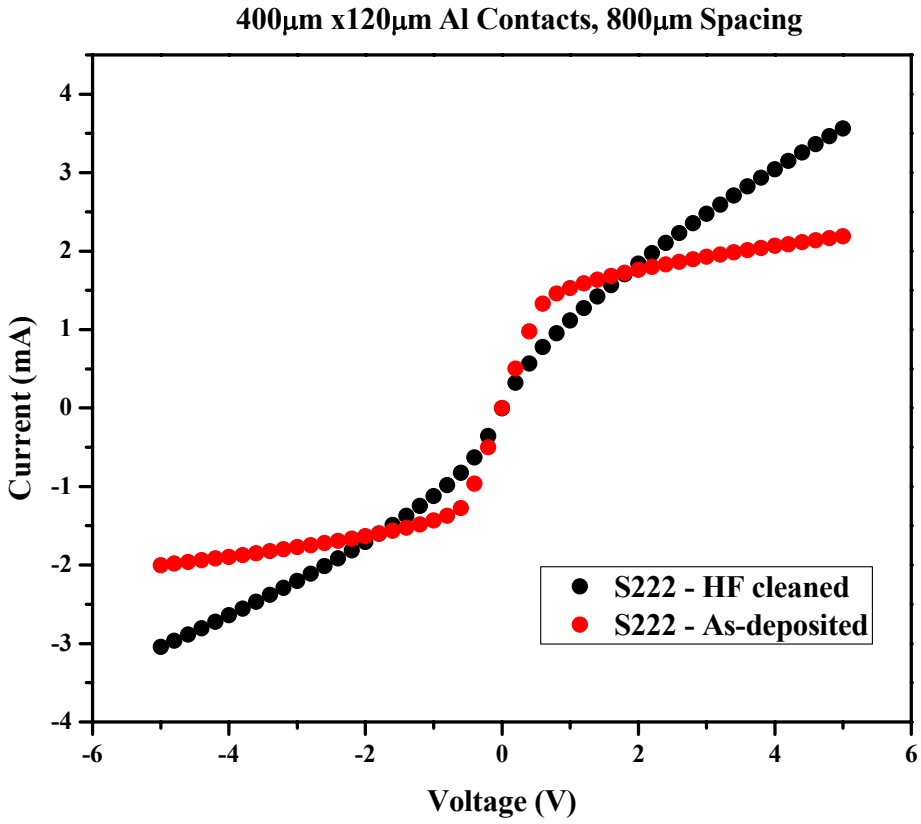

Figure 6.6 - I-V characteristics of β̃SiC/Si (100) Heterostructure.

The I-V characteristics of a β-SiC/Si heterojunction MSM are shown in Fig 6.6**.** Two samples were taken for testing purpose. For the first sample normal procedure of contacts deposition was followed and aluminum contacts were deposited on the surface of the samples. This is referred as As-deposited sample. For the second sample same procedure was followed but prior to the contact deposition, the sample was treated with HF. Then the sample is immediately taken to sputtering station and aluminum contacts were deposited. This is called HF cleaned sample.

Fig 6.6 shows the difference between As-deposited sample and HF cleaned sample. Here HF plays an important role in changing the electrical behavior. The HF converts electrical behavior of the contacts from schottky to near ohmic. The hydrogen atoms in HF interacts with dangling

bonds on the surface of β-SiC film. Since hydrogen is a monovalent bond, so it would terminate the surface dangling bonds and remove those surface states in the bandgap. This effect is common and has been observed in Si surfaces for many years **[Bender, 1994].** But in case of β-SiC films hydrogen induces surface metallization **[Soukiassian, 2004]** which may cause ohmic character as shown in figure 6.6. The angular Si-H-Si bonds formed cause an overlap within the conduction band. This effect narrows the band-gap and lifts the Fermi level leading to the metallic surface.

6.8 IV results of H_2 interaction on nano-thin β-SiC/Si (100)

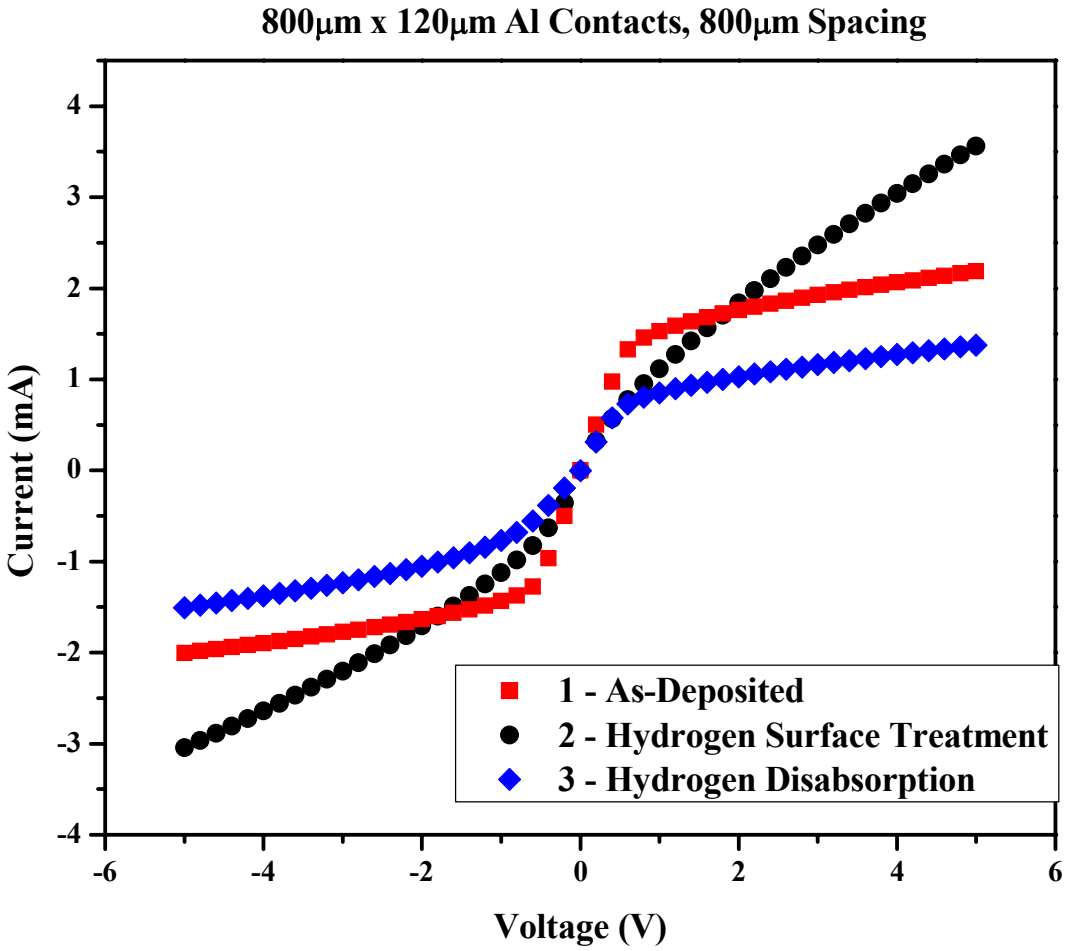

Figure 6.7 - I-V characteristics of β-SiC/Si (100) Heterostructure

The I-V characteristics of a β-SiC/Si heterojunction MSM are shown in Fig 6.7**.** Three samples were taken for testing purpose. For the first sample normal procedure of contacts deposition was followed and aluminum contacts were deposited on the surface of the samples. This is referred as As-deposited sample. For the second sample same procedure was followed but prior to the contact deposition, the sample was treated with HF. Then the sample is immediately taken to sputtering station and aluminum contacts were deposited. This is called Hydrogen Surface Treatment sample. For the third sample same fabrication steps were administered as those for sample 2 except after the hydrogen surface treatment, the sample was placed in a furnace for 3

min at 300^{o}C and then the Al contacts were deposited. Examining the I-V characteristics for sample 3 (Fig. 6.7), it can be seen that the sample has returned to its original as-deposited state. Despite the hydrogen surface treatment, the post heat treatment was successful in removing the hydrogen on the surface of the nano-thin β-SiC layer thus eliminating the metallization. An ideal sensor needs to be recyclable and capable of detecting H_2 continually. So this experiment proves that by heating we can recycle the sample for continual detection of H_2.

6.9 IV results nano-thin β-SiC/Si (100) Vs Temperature

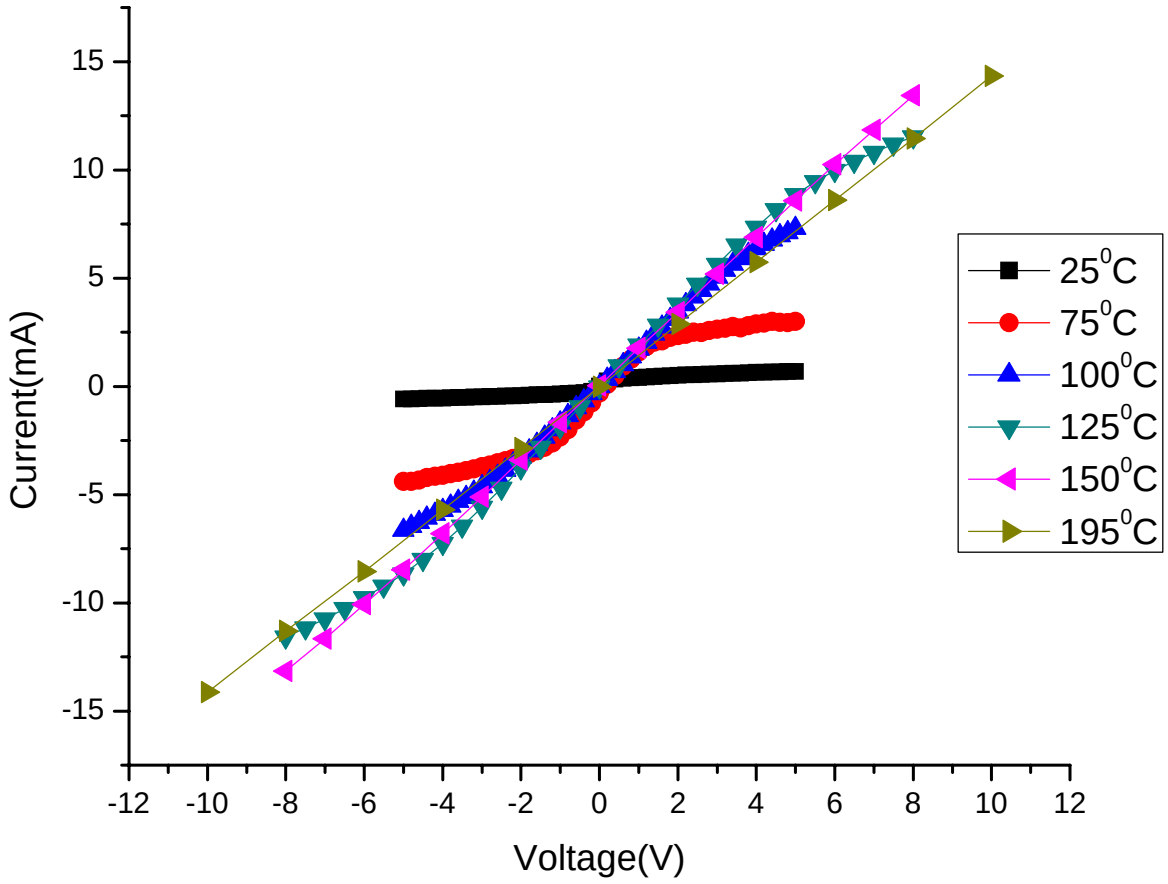

Figure 6.8 I-V characteristics of β-SiC/Si (100) Heterostructure

The I-V characteristics at of a β-SiC/Si heterojunction MSM at different temperatures are shown in Fig 6.8. Aluminum contacts were grown on the sample. The sample is heated from room temperature to 195°c. The I-V characteristic shows that as the electrical behavior of the sample changes to ohmic from schottky with increase in temperature.

6.10 Comparison of IV results β-SiC/Si (100) before and after heating

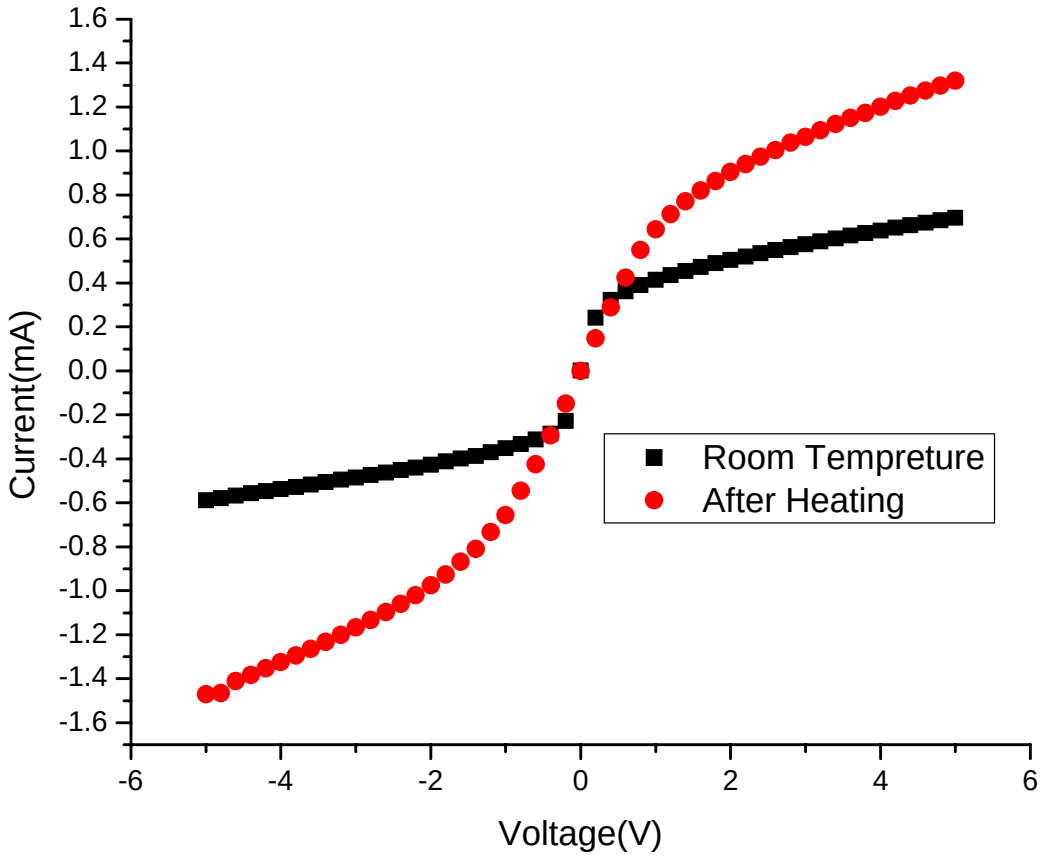

Figure 6.9 I-V characteristics of β-SiC/Si (100) Heterostructure

The I-V characteristics at of a β-SiC/Si heterojunction MSM at room temperature before and after heating are shown in Fig 6.9. Aluminum contacts were grown on the sample. The sample is heated from room temperature to 195^{o}C. Then again it is cooled to room temperature. The I-V characteristics show that there is change in electrical characteristics for sample before and after heating. This is due to the thermally grown Silicon oxide over the sample.

6.11 Change in Current Vs Time for different Hydrogen Percentage for β-SiC/Si

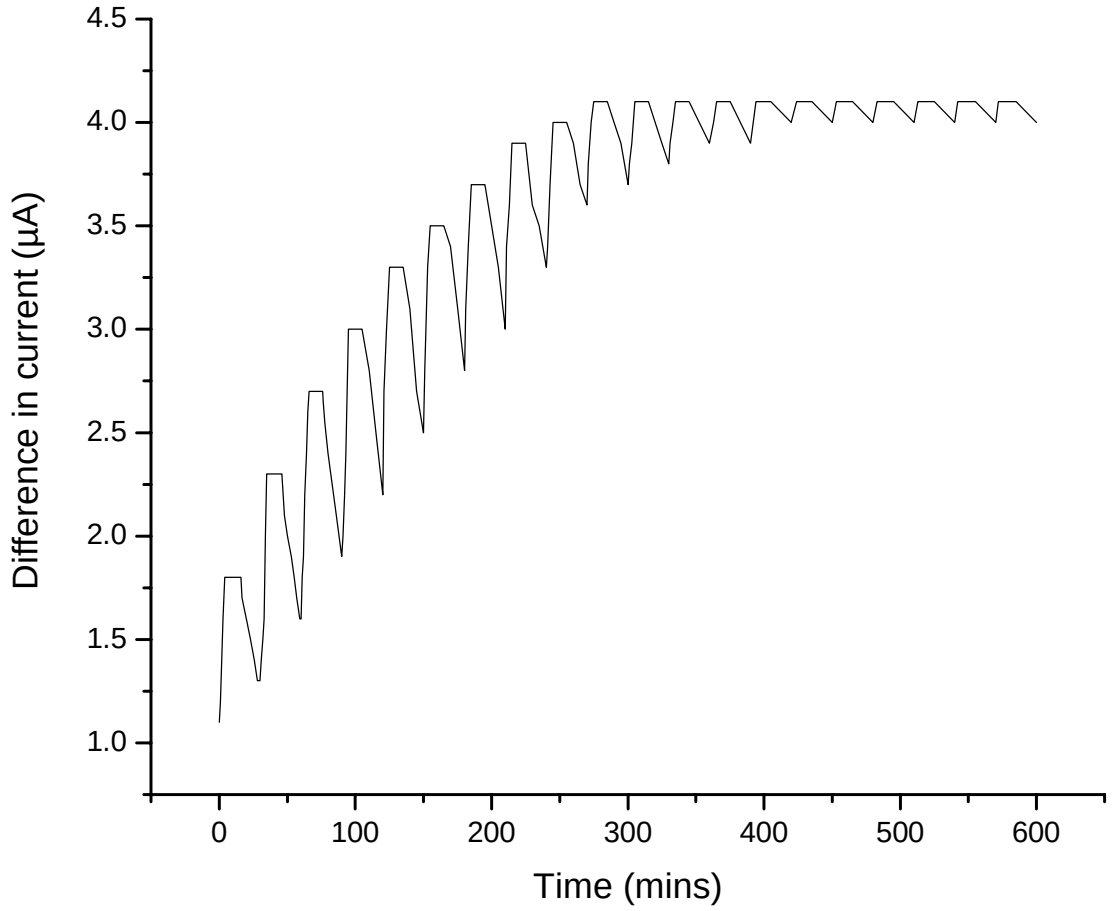

Figure 6.10 Difference in Current for β-SiC/Si at different concentrations of Hydrogen

6.12 Change in Current Vs Hydrogen Percentage for β-SiC/Si (100)

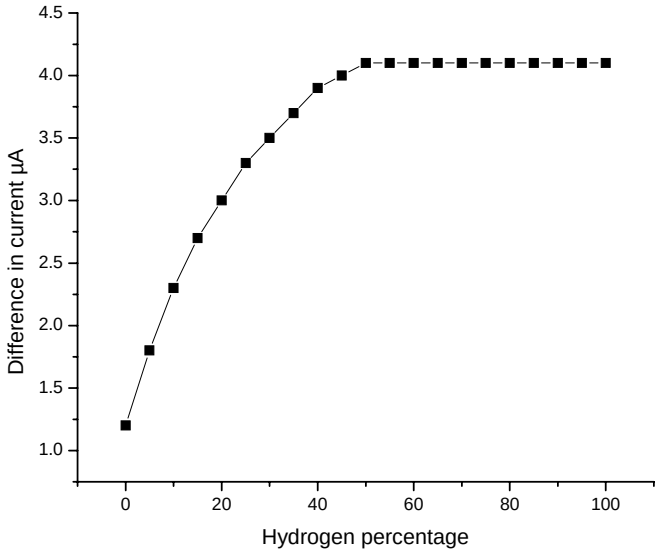

Figure 6.11 Change in Current for β-SiC/Si at different concentrations of Hydrogen.

Fig 6.10 and Fig 6.11 shows change in current for different concentrations of hydrogen of a β-SiC/Si heterojunction. The sample was exposed to different concentrations of hydrogen at room temperature and IV measurements were taken. Argon was flowing continuously through out the process. The electrical characteristics were found to be changing as the flow of hydrogen varies. The current reaches its maximum value within 7 minutes, However, the recovery time is more.

It was observed that as the percentage of hydrogen increases the difference in the current increases. It indicates hydrogen induces surface metallization **[Soukiassian, 2004]** which may cause ohmic character .At some particular concentration of hydrogen the change in current reaches a steady state value. This indicates the saturation point of the sample. Once the hydrogen flow seizes the electrical behavior of sample comes to its original state after a long time.

Chapter 7: Conclusion

Nano-thin β-SiC films were successfully grown on Si substrates. The typical thicknesses of these films were 30nm.For thick β -SiC films (thickness > 3microns), Aluminum contacts exhibits ohmic electrical characteristics. Unlike thick β-SiC films for Nano-thin β -SiC films aluminum contacts exhibits schottky electrical characteristics. This helps in formation of Metal–Semiconductor-Metal heterojunction devices, which acts as solid state gas sensor for detecting hydrogen gas.

A basic Nano-thin β-SiC/Si (100), Metal-Semiconductor-Metal solid state gas sensor was fabricated with aluminum contacts. Changes in the electrical properties were observed when the sample surface is treated with HF. The Metallization of the surface due to the interaction between Si and H bonds is believed to be the cause of the observed increase in current in the presence of hydrogen. Recyclability of the devices was achieved by submitting the sensors to a heat treatment, breaking the H_2 bonds from the surface of the devices.

Changes in electrical properties were also observed when the sample is kept in hydrogen gas chamber. As the concentration of hydrogen gas increases the amount of current increases, indicates the increase in metallization of the surface. Also the electrical property comes back to its original state when the flow of gases seize.

Chapter 8: Future Work

The sensor developed in this work has shown a change in its electrical characteristics in the presence of Hydrogen. Fine tuning the mechanics of the sensor are necessary to maximize its sensitivity and the response time. Increasing the area between adjacent contacts will increase the amount of absorption sites available H_2 detection **[Fawcett, 2004].** Using this effect, the device design of the sensor can be used to optimize the sensitivity of H_2 gas detection. The gas chamber experiment that was performed in this research was carried only at room temperature. Better results can be obtained when the experiment is carried at higher temperatures like temperatures above 250^oC. More over the nano thin β-SiC/Si we used was n-type. If the same experiment was carried on the p-type β-SiC/Si sample we can expect some difference. The β-SiC/Si sensor discussed in this work will need improvements to ensure its successful operation at high temperatures. The use of the non-insulating Si substrate becomes a severe leakage path as carrier concentration increases with rising temperatures. By replacing the Si with a silicon-on-insulator substrate, high isolation can be provided leading to a reduction in leakage current. More recently, it has been shown that chemically etching the Si to obtain porous Si has been effective in obtaining a semi-insulating substrate. **[Hsieh, 2001] [Sagues, 2005]** The high temperature performance of β-SiC devices will need high resistivity substrates to impede the transportation and generation of leakage currents. Operating temperature of β-SiC devices are not limited by the crystal quality, but by the quality of the contact. The testing of different metal/β-SiC systems and their change in electrical properties are needed to ensure high temperature operation. So metals with high melting points must be chosen as contacts for successful operation of nano thin β Silicon carbide at high temperatures.

References

[Andersson, 2004] M. Andersson, H. Petersson, N. Padban, J. Larfeldt, M. Holmberg, A. Lloyd Spetz, "The Characteristics and utility of SiC-FE gas sensors for control of combustion in domestic heating systems." 2004 IEEE Proceedings of sensors, Oct 2004.

[Armgarth, 1982] M. Armgarth, C. Nylander, "Blister Formation in Pd Gate MIS Hydrogen Sensors", IEEE elect. dev. lett., 3, 12, Dec 1982.

[Aroutiounian, 1999] V.M. Aroutiounian, V.V. Buniatyan, P. Soukiassian, " Microwave Characteristics of BARITT diodes Based on Silicon Carbide", IEEE Trans. Elec. Dev., 46, 3, March 1999.

[Baccarani, 1973] G. Baccarani, P.U. Calzolari, S. Graffi, "Current Transport in MSM Devices" Journal of Applied Physics. 45, 1, Jan 1974.

[Baranzahi, 1998] A. Baranzahi, P. Tobias, A.L. Spetz, P. Màrtensson, L. Ekedahi, I. Lundsfröm, "Chemical Sensors with Catalytic Metal Gates" J. Electrochem. Soc., 145, 10, Oct 1998.

[Basu, 2000] S. Basu, S. Roy, R. Laha, C. Jacob, S. Nishino, "Schottky behaviour of Pd β-SiC junctions**"** Optoelectronic and Microelectronic Materials and Devices, 2000. COMMAD 2000. Proceedings Conference 6-8 Dec. 2000, pp: 328–331.

[Bhatnagar, 1996] M. Bhatnagar, B.J. Baliga, H.R. Kirk, G.A. Rozgonyi, "Effect of Surface Inhomogeneities on the Electrical Characteristics of SiC Schottky Contacts" IEEE trans. elect. dev., 43, 1, Jan 1996.

[Bender, 1994] H. Bender, L. Li, P.W. Mertens, M. Meuris, W. Vandervorst, M.M. Heyns, "Surface Passivation and microroughness of (100) silicon etched in aqueous hydrogen halide (HF, HCl, HBr, HI) solutions" J. Appl. Phys., 77, 1 Feb 1995, pp:1323-1325.

[Berger, 1996] P. Berger, "MSM Photodiodes" IEEE Potentials, Apr/May 1996. pp:25-29.

[Bumgarner, 1989] Bumgarner, H.S Kong, H.J Kim, J.W Palmour, J.A Edmond, J.T Glass, R.F Davis, "Monocrystalline β-SiC Semiconductor Thin Films: Epitaxial Growth, Doping, And FET Device Development." Thin Solid Films, 181, 10 Dec. 1989: pp. 1-15

[Campbell, 2001] S. Campbell, "Epitaxial Growth" The Science and Engineering of Microelectronic Fabrication New York: Oxford University Press, 2001: pp. 366-367.

[Chang, 2005] H. Chang, J. Wu, B. Gu, F. Liu, W. Duan, "Physical Origin of Hydrogen-Adsorption-Induced Metallization of the SiC Surface: n-Type Doping via Formation of Hydrogen Bridge Bond" Physical Review Letters, 95, Oct 2005.

[Chaudhry, 1991] M.I. Chaudhry, "Electrical Transport Properties of Crystalline Silicon Carbide/Silicon Heterojunctions**"** IEEE trans. elect. devices, 12, 12, Dec 1991: pp. 670-672.

[Chu, 1971] J.L. Chu, D.J Coleman, S.M. Sze, "Microwave oscillations in p-n-p and metal-n-p BARITT diodes" 1971 International Electron Devices Meeting, 17, 1971.

[Cole, 2002] M.W. Cole, J.D. Demaree, C.W. Hubbard, M.C. Wood, M.H. Ervin, "Novel Ni-Based Ohmic Contacts to n-SiC for High Temperature and High Power Device Applications" High Performance Devices, 2002. Proceedings, 6-8 Aug. 2002, pp: 65-74.

[Coleman, 1972] D.J. Coleman, "Transit-Time Oscillations in BARITT Diodes", J. Appl. Phys., 43, 4, April 1972.

[Cooper, 1997] J.A. Cooper, "Oxides on SiC" 1997 Proceedings of High Speed Semiconductor Devices and Circuits, Aug. 1997.

[Cooper, 2004] J.A. Cooper, "Silicon Carbide Electronic Devices and Integrated Circuits for Extreme Environments", 2004 IEEE Aerospace Conference Proceedings, pp: 2507-2514.

[Davis, 1991] R.F. Davis, G. Kelner, M. Shur, J.W. Palmour, J.A. Edmond, "Thin Film Deposition and Microelectronic and Optoelectronic Device Fabrication and Characterization in Moncrystalline Alpha and Beta Silicon Carbide." Proceedings of the IEEE, 79, 5, May 1991: pp. 677-701.

[Deak, 2002] P. Deak, B. Aradi, A. Gali, U. Gerstmann, "Some like it shallower – p-type doping in SiC" phys. stat. sol., 235, dec 2002, pp: 139-145.

[Fawcett, 2004] T.J. Fawcett, J.T. Wolan, R.L. Myers, J. Walker, S.E. Saddow, "Wide-range (0.33%-100%) 3C-SiC resistive hydrogen gas sensor development" Appl. Phys. Lett., 85, 3, 19 Jul 2004.

[Fukuda, 2000] K. Fukuda, W.J. Cho, K. Arai, "Effect of oxidation method and post-oxidation annealing on interfaces properties of metal-oxide-semiconductor structures formed on n-type 4H-SiC C(0001) face", Applied Physics Letters, 77, 6, 7 Aug 2000.

[Ghosh, 2002] R.N. Ghosh, P. Tobias, S.G. Ejakov, B. Golding, "Interface States in High Temperature SiC Gas Sensing" Sensors 2002. Proceedings of IEEE, 2, 12-14 Jun. 2002, pp: 1120-1125.

[Grinberg, 1989] A.A. Grinberg, S. Luryi, M.R. Pinto, N.L. Schryer, "Space-Charge-Limited Current in a Film" IEEE trans. elect. dev., 36, 6, Jun. 1989.

[Hsieh, 2001] W.T Hseih, Y.K Fang, K.H Wu, W.J Lee, J.J Ho, C.W Ho, "Using porous Silicon as Semi-Insulating Substrate for β–SiC High Temperature Optical-Sensing Devices**"** IEEE trans. elect. dev, 48, 2, Feb 2001: pp. 801-803.

[Hwang, 1997] J.D. Hwang, Y.K. Fang, K.H. Wu, S.M. Chou, "Improving Breakdown Voltage of SiC/Si Heterojunction with Graded Structure by Rapid Thermal CVD Technology" IEEE trans. elect. dev., 44, 11, Nov. 1997.

[Hwu, 1993] R.J. Hwu, A. Djuandi, S.C. Lee, "Negative Differential Resistance (NDR) Frequency Conversion with Gain" IEEE trans. microwave theory, 41, 5, May 1993.

[Jin, 2006] N. Jin, S. Guosheng, G. Quancheng, L. Zhongli, "Fabrication of Poly Crystalline 3C-SiC Resonator" 2006 Solid-State and Integrated Circuit Technology, Oct. 2006, pp: 938-940.

[Kakanakov, 2002] R. Kakanakov, L. Kassamakova-Kolaklieva, N. Hristeva, G. Lepoeva, K. Zekentes, "Thermally Stable Low Resistivity Ohmic Contacts for
High Power and High Temperature SiC Device Applications" PROC. 23rd INTERNATIONAL CONFERENCE ON MICROELECTRONICS (MIEL 2002), 1, 12-15 May, 2002.

[Kasap, 2001] S.O. Kasap, " PN Junction Principles " Optoelectronics and Photonics. Upper Saddle River, New Jersey: Prentice-Hall, Inc, 2001.

[Kim, 2001] C.K. Kim, J.H. Lee, S.M. Choi, I.H. Noh, H.R. Kim, N.I. Cho, C. Hong, G.E. Jang, "Pd- Pt-SiC Schottky diodes for detection of H_2 and CH_4 at high temperature" Sensors and actuators B, 77, 2001, pp: 455-462.

[Loloee, 2005] R. Loloee, R.N. Ghosh, "Performance of Silicon Carbide High Temperature Gas Sensors" 2005 IEEE Sensors, 2005.

[Lu, 1993] J. Lu, R. Surridge, G. Pakulski, H. Driel, J.M. Xu, "Studies of High-Speed Metal-Semiconductor-Metal Photodector with a GaAs/AlGaAs/GaAs Heterostructure" IEEE trans. elect. dev., 40, 6, Jun 1993.

[Morales, 2002] F.M. Morales, S.I. Molina, D. Araujo, V. Cimalla, J. Pezoldt, L. Barbadillo, M.J. Hernandez, J. Piqueras, "Transmission electron microscopy study of ultra-thin SiC layers obtained by rapid thermal carbonization of Si wafer" phys. stat. sol., 195, 1, 2003, pp: 116-121.

[More, 2003] K.L. More, P.F. Tortorelli, L.R. Walker, N. Miriyala, J.R. Price, M. van Roode, "High-Temperature Stability of SiC-Based Composites in High-Water-Vapor-Pressure Environments" J. Am. Ceram. Soc., 86, 2003, pp: 1272-1281.

[Matsunami, 1981] H. Matsunami, S. Nishino, H. Ono, "IVA-8 heteroepitaxial growth of cubic silicon carbide on foreign substrates**"** IEEE trans. elect. devices, 28, 10, Oct 1981: pp. 1235-1236.

[Muller, 2002] R.S Muller, T.I Kamins, "Metal-Semiconductor Contacts" Device Electronics for Integrated Circuits New York: John Wiley & Sons, 2002: pp. 162-165.

[Nabet, 1997] B. Nabet, "A Heterojunction Metal-Semiconductor-Metal Photodetector" IEEE Photonics Tech. Let. 9, 2, Feb 1997.

[Nabet, 2001] B. Nabet, F. Quaranta, A. Cola, "Heterojunction and Heterodimensional Devices for Optoelectronics" 2001 IEEE Microwave, Mar. 2001.

[Neudeck, 1994] P.G. Neudeck, "Progress in Silicon Carbide Semiconductor Electronics Technology" Journal of Electronic Materials, 24, 4, 1995.

[Neudeck, 2001] P. G. Neudeck, "Silicon Carbide Electronic Devices," Encyclopedia of Materials: Science and Technology, 9, Eds. Oxford: Elsevier Science, 2001: pp. 8508-8519.

[Nishino, 1987] S. Nishino, J. Suhara, H. Ono, H. Matsunami, "Epitaxial growth and electric characteristics of cubic SiC on silicon" J. Appl. Phys., 61, 15 May 1987.

[Ohn, 2006] C.M. Ohn, G.S. Chung, "Ohmic Contacts of Polycystalline 3C-SiC Thin-Films Grown on Si (100) Wafers for Microsensors of Vehicle Engines" The 1st International Forum on Strategic Technology, Oct. 2006, pp: 301-304.

[Oyabu, 1981] T. Oyabu, "Sensing characteristics of SnO_2 thin film gas sensor", American Institute of Physics, 53, April 1982.

[Palmour, 1988] J.W. Palmout, H.S. Kong, R.F. Davis, "Characterization of device parameters in high-temperature metal-oxide-semiconductor field-effect transistors in β-SiC thin films" J. Appl. Phys., 84, 4, 15 Aug. 1988.

[Pearton, 2004] S.J. Pearton, B.S. Kang, S. Kim, F. Ren, B.P. Gila, C.R. Abernathy, J. Lin, S.N. Chu, "GaN-based diodes and transistors for chemical, gas, biological and pressure sensing" J. Phys. Condens. Matter, 16, 2004.

[Peng, 2006] X. Peng, J. Pollmann, P. Kruger, "Hydrogen-induced metallization of the 3C-SiC(001)-(3×2) surface" Surface Science, 600, 18, 15 Sept. 2006, pp: 3564-3569.

[Porter, 1995] L.M Porter, R.F Davis, "A Critical Review of Ohmic and Schottky Contacts for Silicon Carbide**"** Material Science and Engineering. Solid State Materials for Advanced Engineering, 34, 2, May 1995: pp. 83-104.

[Powell, 2002] A.R Powell, L.B. Rowland, "SiC Materials – Progress, Status, and Potential Roadblocks" Proc. IEEE, 90, 6, Jun. 2002.

[Roy, 2003] S. Roy, C. Jacob, S. Basu, "Studies on Pd/3C-SiC Schottky junction hydrogen sensors at high temperature" Sensors and Actuators – B Chemical, 94, 17 Apr 2003.

[Sagues, 2005] A.A. Sagues, J.T. Wolan, A.D. Fex, T.J. Fawcett, "Impedance behavior of nanoporous SiC" Electrochimica Acta, 51, 2006, pp: 1656-1663.

[Sasaki, 1984] K.Sasaki, E. Sakuma, S. Misawa, S. Yoshida, S. Gonda, "High-temperature electrical properties of 3C-SiC epitaxial layers grown by chemical vapor deposition." Appl. Phys. Lett, 45, 1 July 1984: pp. 72-73.

[Sayago, 2002] I. Sayago, M.C. Horrillo, S. Baluk, M. Aleixandre, M.J. Fernandez, L. Ares, M. Garcia, J.P. Santos, J. Gutierrez, "Detection of Toxic Gases by a Tin Oxide Multisensor", IEEE Sensors Journal, 2, 5, Oct 2005

[Scholz, 1998] R.Scholz, U. Gosele, F. Wischmeyer, E. Niemann,"Prevention of micropipes and voids at β-SiC/Si(100) interfaces." Appl .Phys. A, 66, 30 Jul 1997: pp. 59-67.

[Silly, 2004] M.G. Silly, C. Radtke, H. Enriquez, P. Soukiassian, "Hydrogen-induced metallization of a preoxidized 3C-SiC(100)3x2 surface" Appl. Phys. Lett., 85, 11, 22 Nov. 2004.

[Steadman, 2000] J.W. Steadman. "Section III – Electronics" The Electrical Engineering Handbook. Ed. Richard C. Dorf. Boca Raton: CRC Press LLC, 2000.

[Streetman, 2003] B.G Streetman, S. Banerjee, "Junctions" Solid State Electronic Devices New Delhi: Prentice-Hall of India, 2003: pp. 226.

[Sze, 1971] S.M Sze, D.J Coleman, A. Loya, "Current Transport in Metal-Semiconductor-Metal (MSM) Structures" Solid-State Electron. 14, 1209. 1971.
[Sze, 1981] S.M Sze, "Metal-Semiconductor Contacts" Physics of Semiconductor Devices New York: John Wiley & Sons, 1981: pp. 275-276.

[Taur, 2005] Y. Taur, T.H Ning, "Basic Device Physics" Fundamentals of Modern VLSI Devices New York: Cambridge University Press, 2005: pp. 83-84.

[Tobias, 1997] P. Tobias, A. Baranzahi, A.L. Spetz, O. Kordina, E. Janzen, I. Lundstrom, "Fast Chemical Sensing with Metal-Insulator Silicon Carbide Structures" IEEE Elec. Dev. Lett., 18, 6, June 1997.

[Tobias, 2003] P. Tobias, B. Golding, R.N. Ghosh, "Interface States in High-Temperature Gas Sensors Based on Silicon Carbide" IEEE Sensors Journal, 2, 5, Oct 2003.

[Tung, 1991] R.T. Tung, "Electron transport of inhomogeneous Schottky barriers" Appl. Phys. Lett., 58, 24, 17 Jun. 1991.

[Wan, 2002] J. Wan, M.A. Capano, M.R. Melloch, J.A. Cooper, "Inversion Channel MOSFETs in 3C-SiC on Silicon" IEEE elec. dev. lett., 23, 8, Aug 2002.

[Wasa, 2001] K.Wasa, "Thin Film Technology As A Materials Engineering" Revista Brasileira de Aplicacoes de Vacuo, 20, 1, 2001.

[Weyher, 2006] J.L. Weyher, "Characterization of wide-band-gap semiconductors (GaN, SiC) by defect-selective etching and complementary methods", Elsevier Supperlattices and Microstructures, 40, 8 Aug 2006, pp: 279-288.

[Yano, 1999] H. Yano, F. Katafuchi, T. Kimoto, H. Matsunami, "Effects of Wet Oxidation/Anneal on Interface Properties of Thermally Oxidized SiO_2/SiC MOS System and MOSFET's", IEEE trans. elect. dev., 46, 3, March 1999, pp: 504-510.

[Yeh, 1985] C. Yeh, "A Planar Back-To-Back Schottky-Barrier Photodiode" Proceedings of The IEEE, 73, 2, Feb 1985.

[1] "Thermal Conductivity Table" Georgia State University 2007 <http://hyperphysics.phy-astr.gsu.edu/hbase/tables/thrcn.html>

[2] "NSM Archive – Physical Properties of Semiconductors." Ioffe Physico-Technical Institute 2007 <http://www.ioffe.rssi.ru/SVA/NSM/Semicond/index.html>

APPENDIX A:

PROTOCOL FOR SAMPLE CLEANING

1. Place sample in Petri dish,
2. Fill the Petri dish with acetone and leave it for 5 minutes
3. Remove sample and place in another Petri dish,
4. Fill the Petri dish with methanol and leave it for 5 minutes
5. Blow dry sample with N_2 gas

APPENDIX B:

PROTOCOL FOR OXIDE DEPOSITION

1. Turn on Nitrous gas, and plug in respective valve heater
2. Turn on Silane gas, and open LPI valve and HPI valve
3. Turn on gas monitor, and open valve
4. On PECVD computer program, set substrate temperature to 300^{o}C
5. Once temperature reads 300^{o}C, vent system
6. Hoist lid up using controls on the front of the chamber
7. Load sample onto PECVD substrate
8. Hoist lid down using controls on the front of the chamber
9. On PECVD computer program, under 'current action', select process
10. Under select menu, select the "SiO_x 4.5 min" process (yields 300nm)
11. Select 'display' select 'status' to 'start'
12. Once the process is complete, Hoist lid up using controls on the front of the chamber
13. Unload sample from PECVD substrate
14. Hoist lid down using controls on the front of the chamber
15. Select 'manual', then set temperature to 0^{o}C, select 'manual'-> 'vacuum' -> 'start'
16. Turn off Nitrous gas, and unplug the respective valve heater
17. Turn off Silane gas, and close LPI valve close HPI valve
18. On gas monitor, and close valve

APPENDIX C:

PROTOCOL FOR IMAGE REVERSAL LITHOGRAPHY

1. Place sample in spinner and turn on vacuum to secure sample to platform
2. Use pipette to deposit a bead of AZ5214 photo resist on the surface of the sample
3. Set the spinner to 4000 RPM for a time of 50 seconds and select 'start'
4. After spinner has stopped, turn off vacuum and remove sample
5. Place sample on hot plate, set to a temperature of 90^{o}C for 45 seconds
6. Perform lamp test to determine the power and then calculate the exposure time using formula below:

$$t(\text{sec}) = \frac{130(mJ/cm^2)}{power(mW/cm^2)}$$

7. Place sample on stage of Karl Suss MA6 aligner
8. Expose the sample in the Aligner using the time calculated
9. Load contact mask in Aligner
10. Remove sample from aligner stage and place on hot plate, set to a temperature of 115^{o}C for 2 minutes.
11. Remove sample and place under flood exposure for 82 seconds
12. Place sample in beaker filled with (6 parts H_2O: 1 part AZ 400K developer) for 2 minutes
13. Place sample in beaker filled with water for 30 seconds
14. Blow dry with nitrogen gas

APPENDIX D:

PROTOCOL FOR BUFFERED OXIDE ETCH (BOE)

1. Fill Nalgene beaker with Buffered Oxide Etch (BOE)
2. Calculate etch rate based on: 143nm/min
3. Secure sample in plastic holder and deposit into BOE solution
4. Remove sample from BOE solution and place into a Nalgene beaker filled with water
5. Continuously cascade water over sample for 10 minutes
6. Dispose of BOE solution by using aspirator and then continuously cascading water in beaker for 10 minutes
7. After sample has been diluted in water for 10 minutes, blow dry with Nitrogen gas

APPENDIX E:

PROTOCOL FOR METAL DEPOSITION

1. Turn on Argon gas
2. Select “Vent” on control panel
3. Once vacuum light turns off, hoist lid of sputtering station
4. Mount sample onto bracket and place in station 3
5. Lower lid of sputtering station
6. Select “Mechanical Pump” and then “Rough valve”
7. Pump down chamber until pressure reads 1
8. Turn off “Rough Valve” and Turn on “Hivac”
9. Pump down chamber until flow controller reads two decimal places
10. Turn on Ion Gauge and wait until it reads 5.0×10^{-6}
11. Set the sputtering time to 1.8 minutes on master count module
12. Close the throttle valve
13. Turn on Gas 1
14. Adjust throttle valve until Argon pressure reads 6.00
15. Switch on power for station 4
16. Check the target power is set to 0.1KW
17. Turn on continuous switch on interlock controller
18. Turn on MDX panel and wait 1 minute as a pre-deposition is performed
19. After 1 minute, simultaneously switch on timer and open shutter to station 4
20. After deposition, turn off MDX panel
21. Turn off Gas 1
22. Open the throttle valve
23. Turn off HIVAC
24. Select “Vent” on control panel
25. Remove sample from bracket
26. Hoist down the lid
27. Select “Mechanical Pump” and then “Rough valve”
28. Turn off Argon gas

APPENDIX F:

PROTOCOL FOR METAL LIFT-OFF

1. Place sample in Petri dish, half filed with acetone for 5 minutes
2. Place Petri dish inside ultrasonic bath, and pulse repeatedly at 3 sec intervals until excess metal has been removed from the sample's surface
3. Place sample in Petri dish,
4. Fill the Petri dish with acetone and leave it for 5 minutes
5. Remove sample and place in another Petri dish,
6. Fill the Petri dish with methanol and leave it for 5 minutes
7. Blow dry sample with N_2 gas

APPENDIX G:

PROTOCOL FOR CONTACT DEPOSITION

1. Follow PROTOCOL FOR SAMPLE CLEANING
2. Follow PROTOCOL FOR OXIDE DEPOSITION
3. Follow PROTOCOL FOR IMAGE REVERSAL LITHOGRAPHY
4. Follow PROTOCOL FOR ETCHING USING BUFFERED OXIDE ETCH
5. Follow PROTOCOL FOR METAL DEPOSITION
6. Follow PROTOCOL FOR METAL LIFT-OFF

APPENDIX H:

PROTOCOL FOR ANNEALING

1. Set the Thermolyne furnace to the desired temperature
2. Turn on the N_2 gas supply
3. Wait until the furnace has reached the desired temperature (300^oC)
4. Place the sample onto the dish holder and insert it inside the furnace
5. Leave the sample inside the furnace for 2 min
6. Remove the sample and let cool for 10 min
7. Turn off N_2 gas supply